

Alma Mater Studiorum Università di Bologna
Archivio istituzionale della ricerca

Increasing market opportunities for renewable energy technologies with innovations in aquifer thermal energy storage

This is the final peer-reviewed author's accepted manuscript (postprint) of the following publication:

Published Version:

Hoekstra N., Pellegrini M., Bloemendal M., Spaak G., Andreu Gallego A., Rodriguez Comins J., et al. (2020). Increasing market opportunities for renewable energy technologies with innovations in aquifer thermal energy storage. SCIENCE OF THE TOTAL ENVIRONMENT, 709, 1-18 [10.1016/j.scitotenv.2019.136142].

Availability:

This version is available at: <https://hdl.handle.net/11585/715271> since: 2024-06-11

Published:

DOI: <http://doi.org/10.1016/j.scitotenv.2019.136142>

Terms of use:

Some rights reserved. The terms and conditions for the reuse of this version of the manuscript are specified in the publishing policy. For all terms of use and more information see the publisher's website.

This item was downloaded from IRIS Università di Bologna (<https://cris.unibo.it/>).
When citing, please refer to the published version.

(Article begins on next page)

Increasing market opportunities for renewable energy technologies with innovations in aquifer thermal energy storage

Hoekstra, N.; Pellegrini, M.; Bloemendal, M.; Spaak, G.; Andreu Gallego, A.; Rodriguez Comins, J.; Grotenhuis, T.; Picone, S.; Murrell, A. J.; More Authors

DOI

[10.1016/j.scitotenv.2019.136142](https://doi.org/10.1016/j.scitotenv.2019.136142)

Publication date

2020

Document Version

Accepted author manuscript

Published in

Science of the Total Environment

Citation (APA)

Hoekstra, N., Pellegrini, M., Bloemendal, M., Spaak, G., Andreu Gallego, A., Rodriguez Comins, J., Grotenhuis, T., Picone, S., Murrell, A. J., & More Authors (2020). Increasing market opportunities for renewable energy technologies with innovations in aquifer thermal energy storage. *Science of the Total Environment*, 709, Article 136142. <https://doi.org/10.1016/j.scitotenv.2019.136142>

Important note

To cite this publication, please use the final published version (if applicable).
Please check the document version above.

Copyright

Other than for strictly personal use, it is not permitted to download, forward or distribute the text or part of it, without the consent of the author(s) and/or copyright holder(s), unless the work is under an open content license such as Creative Commons.

Takedown policy

Please contact us and provide details if you believe this document breaches copyrights.
We will remove access to the work immediately and investigate your claim.

1 Increasing market opportunities for 2 renewable energy technologies with 3 innovations in 4 aquifer thermal energy storage

5 N. Hoekstra^{1*}, M. Pellegrini², M. Bloemendal³, G. Spaak¹, A. Andreu Gallego⁴, J. Rodriguez Comins⁵, T. Grotenhuis⁶, S.
6 Picone⁷, A.J. Murrell⁸, H.J. Steeman⁹, A. Verrone¹⁰, P. Doornenbal¹¹, M. Christophersen¹², L. Bennedsen¹², M. Henssen¹³,
7 S. Moinier¹⁴, C. Saccani²

8 ¹*Department of Soil & Groundwater Quality, Deltares, Utrecht, The Netherlands.*

9 ²*Department of Industrial Engineering, University of Bologna, Bologna, Italy.*

10 ³*Department of Water Management, Delft University of Technology, Delft, The Netherlands & KWR Watercycle research*
11 *institute, Nieuwegein, The Netherlands.*

12 ⁴*Sustainability Department, Ceramic Technology Institute, Castellon de la Plana, Spain.*

13 ⁵*Itecon, Castellon de la Plana, Spain.*

14 ⁶*Sub-Department of Environmental Technology, Wageningen University, Wageningen, The Netherlands.*

15 ⁷*ART-ER, Research and Innovation Division, Bologna, Italy*

16 ⁸*Naked Energy Limited, Crawley, United Kingdom.*

17 ⁹*Arcadis Belgium nv/sa, Gent, Belgium.*

18 ¹⁰*NE Nomisma Energia s.r.l., Bologna, Italy.*

19 ¹¹*Department of Applied Geology & Geophysics, Deltares, Utrecht, The Netherlands.*

20 ¹²*Department of Contaminated Soil & Groundwater, Ramboll, Vejle, Denmark.*

21 ¹³*Bioclear Earth, Groningen, The Netherlands.*

22 ¹⁴*Department of Urban Water & Subsurface, Deltares, Utrecht, The Netherlands.*

23 **Corresponding author.*

24 **Abstract**

25 Heating and cooling using aquifer thermal energy storage (ATES) has hardly been applied outside the Netherlands, even
26 though it could make a valuable contribution to the energy transition. The Climate-KIC project “Europe-wide Use of
27 Energy from aquifers” – E-USE(aq) – aimed to pave the way for Europe-wide application of ATES, through the
28 realization and monitoring of six ATES pilot plants across five different EU countries. In a preceding paper, based on
29 preliminary results of E-USE(aq), conclusions were already drawn, demonstrating how the barriers for this form of
30 shallow geothermal energy can be overcome, and sometimes even leveraged as opportunities. Based on final pilot project
31 results, key economic and environmental outcomes are now presented. This paper starts with the analysis of specific
32 technological barriers: unfamiliarity with the subsurface, presumed limited compatibility with existing energy provision
33 systems (especially district heating), energy imbalances and groundwater contamination. The paper then shows how these
34 barriers have been tackled, using improved site investigation and monitoring technologies to map heterogeneous subsoils.
35 In this way ATES can cost-efficiently be included in smart grids and combined with other sources of renewable (especially
36 solar) energy, while at the same time achieving groundwater remediation. A comparative assessment of economic and
37 environmental impacts of the pilots is included, to demonstrate the sustainability of ATES system with different
38 renewables and renewable-based technologies. The paper concludes with an assessment of the market application
39 potential of ATES, including in areas with water scarcity, and a review of climate beneficial impact.

40

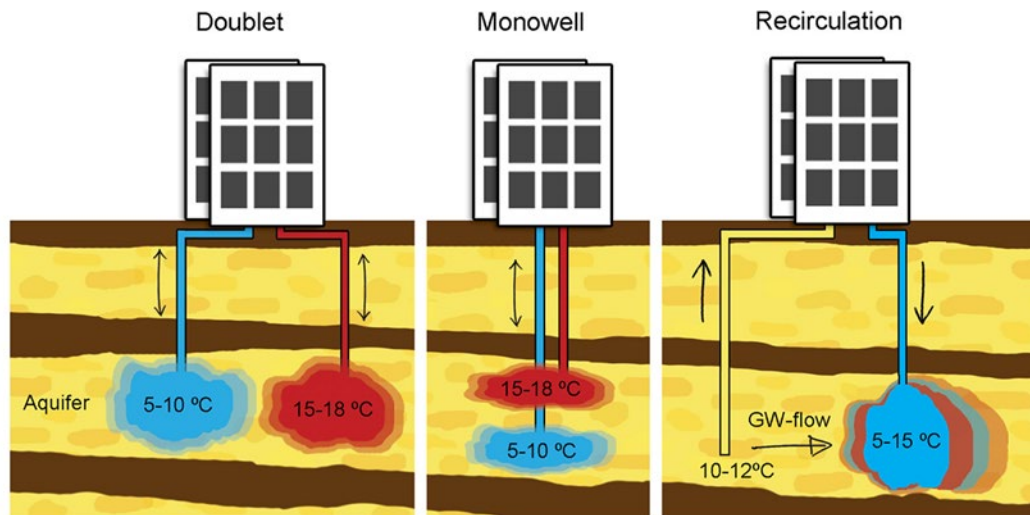
41 **Keywords:** geothermal energy, aquifer thermal energy storage, heating and cooling, pilot plant, technological innovation,
42 remediation, district heating and cooling, photovoltaic-thermal module, water scarcity.

43

44 **1. Introduction**

45 A transition to a low carbon energy system is needed to respond to the global challenge of climate change. Aquifer
46 Thermal Energy Storage (ATES) is a technology with worldwide potential to provide sustainable space heating and
47 cooling by (seasonal) storage and recovery of heat in the subsurface (Bloemendal et al., 2015). The basic working
48 principle of ATES is described in Pellegrini et al., 2019a. Figure 1 shows schematics of three main design types.

49



50

51 Figure 1. Schematic representation of ATES doublet, monowell and recirculation systems. The doublet system at the left is the most
 52 common. The monowell system in the middle, with the hot well on top of the cold well needs less space and has lower installation
 53 costs, since one borehole suffices. The recirculation system is preferable at high groundwater flows but is less effective, since infiltrated
 54 cold and heat are not reused.

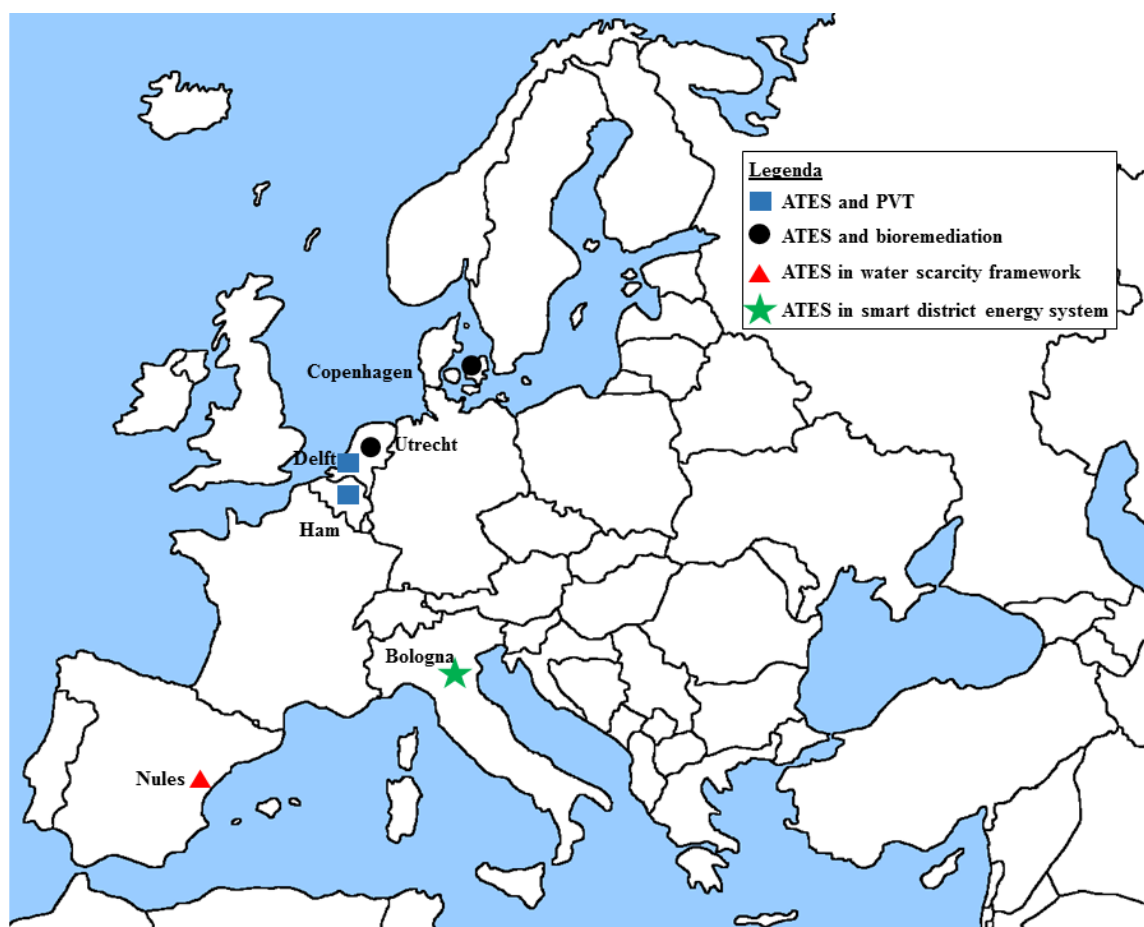
55

56 Various ATES systems have been reported in operation for heating and cooling supply (Bertani, 2005; Gao et al., 2017;
 57 Fleuchaus et al., 2018): ATES have been developed and widely applied in the Netherlands in the last few decades, while
 58 this technology has been only recently picked up also in other countries, such as Belgium, Denmark, Germany, Sweden
 59 and the US. As a result, more than 2800 ATES are installed worldwide, but more than 90% are operating in the
 60 Netherlands alone. ATES reaches the highest efficiency if applied in buildings with high, constant and balanced energy
 61 demand over the year, such as offices, airports, universities, shopping malls and hospitals (Fleuchaus et al., 2018). Despite
 62 the high market potential, the adoption of ATES across Europe has been slow, mainly because of technical (building,
 63 subsurface and climatic conditions) and organizational/legal barriers (Haehnlein et al, 2010; Monti et al., 2012; Pellegrini
 64 et al., 2019a). Economic barriers are also present: though some feasibility studies can be found in literature (Schüppler et
 65 al., 2019), the majority of the studies only briefly summarised the economics of ATES.

66 After identification and classification of all of these barriers in the Climate-KIC project ‘Europe-wide Use of Sustainable
 67 Energy from aquifers’ – E-USE(aq) – the project team demonstrated how the barriers can be overcome by implementing
 68 six ATES pilot systems across five different EU-countries (Pellegrini et al., 2019a). At two sites (Delft-The Netherlands
 69 and Ham-Belgium) ATES has been integrated with hybrid photovoltaic or photovoltaic-thermal (PVT) panels, thus
 70 addressing the gaps of heating/cooling demand seasonal balancing and of heat pumps power consumption. At two other
 71 sites ATES has been combined with bioremediation (Utrecht-The Netherlands and Birkerød, Greater Copenhagen-
 72 Denmark) to demonstrate how ATES can be effectively applied in contaminated sites for bioremediation purposes. At a

73 Spanish site (Nules), located within an area affected by water scarcity, a system without groundwater extraction and
 74 infiltration has been installed in a swimming-pool. Finally, in an Italian site (Anzola dell’Emilia, Bologna) a recirculation
 75 ATEs system has been realized to feed a small district heating and cooling network, to verify how ATEs systems can be
 76 integrated in smart district energy grids. Figure 2 shows a map of the pilot plants locations, while in Table 1 a summary
 77 of main pilot plant data is given. More information about the pilot plants can be found in Pellegrini et al., 2019a and in
 78 the provided supplementary material.

79



80

81

Figure 2. Map distribution of E-USE(aq) project pilot plants.

82

83

Table 1. Pilot plants main characteristics. (*) extraction and injection wells.

Parameter	Delft	Utrecht	Copenhagen	Ham	Bologna	Nules
N° of production wells (*)	1 + 1	3 + 3	1 + 1	1 + 1	3 + 3	4
N° of monitoring wells	6	3	4	2	4	4
Wells' depth (m)	60-80	15-55	22-55	162.5	30	35
Max groundwater flowrate (m ³ /h)	25	45	5	80	19.4	14.4

Max cooling power (kW)	30	-	No cooling	1,300	140	No cooling
Max heating power (kW)	70	-	No heating	650	160	109
Annual cooling demand (MWh)	160	-	No cooling	900	49	No cooling
Annual heating demand (MWh)	160	-	No heating	863	170	288

84

85 In Pellegrini et al., 2019a the outcomes of the barrier analysis and preliminary results of the pilot plants were discussed
86 and solutions for overcoming the barriers were presented. The main topics addressed in previous research are reported
87 below:

- 88 - Legislation: In earlier work Haehnlein et al. made an inventory of ATES legislation (Haehnlein et al., 2010).
89 Legislation varies from country to country, all using the precautionary principle as a basis. Barriers indicated and
90 discussed in this work are: poorly substantiated legislation in Spain, a lack of legislation on combining ATES with
91 remediation in Netherlands and Denmark, and complex regulation and poor expertise at the local government level in
92 Italy.
- 93 - Groundwater quality: Two research programs on the effects of ATES on groundwater quality were landmark studies
94 (Koenders, 2015; Bonte, 2015), concluding that low temperature ATES systems like the ones discussed in this paper
95 have negligible effects on groundwater quality. Nevertheless, many research questions remain on how larger
96 temperature changes (> 30°C) affect groundwater quality, as well as how mixing of various groundwater qualities
97 affects aquifer quality. This paper discusses how ATES can be combined with soil/groundwater remediation in
98 Netherlands and Denmark.
- 99 - System design/integration: The Dutch industry organization developed design standards, mainly focusing on avoiding
100 well clogging and on integration of the ATES wells and heat pump into the building system (NVOE, 2006). Earlier
101 and recent work of Doughty et al., Sommer et al. and Bloemendal and Hartog. (Doughty et al., 1982; Sommer et al.,
102 2015; Bloemendal and Hartog, 2018) provided a theoretical basis for optimal use of subsurface space and how to deal
103 with specific geohydrological conditions (e.g. groundwater flow, high density use of ATES, heterogeneity). In this
104 work, further steps are taken in the integration with the buildings system with solar collectors for energy balance (in
105 Belgium and The Netherlands) and integration with district heating (in Italy).

106 The main objective of this follow-up paper is to present the key project results reached in the last year of pilot operations,
107 which offer opportunities to enhance market uptake of ATES and pave the way for a larger scale adoption. In particular,
108 results showed that i) improved site investigation and monitoring technologies can be effectively used to map
109 heterogeneous subsoils, ii) ATES systems can be combined with other sources of renewable energy (especially solar) to

110 balance the energy demand over the years, iii) ATES systems can be designed to be included in smart grids and iv) ATES
111 systems can be effectively combined with groundwater remediation applications. A comparative assessment of economic
112 and environmental impacts of the pilots is included to demonstrate the sustainability of ATES system with different
113 renewables and renewable-based technologies. E-USE(aq) project demonstrated that ATES systems can be applied under
114 strongly varying conditions in different European countries and through different innovative technological solutions.
115 Nevertheless, further continued investigations with long-term monitoring and evaluation of projects are needed to
116 strengthen the results, including economic perspectives.

117

118 **2. Methods & Materials**

119 This chapter includes a description of the methods applied in the design, monitoring and assessment phases of the pilot
120 plants.

121

122 **2.1 Detailed underground characterizations through monitoring actions**

123 One of the main technological barriers identified by E-USE(aq) project is the unfamiliarity with the subsurface (Pellegrini
124 et al., 2019a). This barrier is relevant in both design and monitoring phases, and can have a negative impact also in the
125 authorization/permit phase. For example, when well screens are situated in more than one water bearing layer, water of
126 different composition often mixes, which can result in chemical precipitation of for instance iron oxides or sulphides and
127 consequently clogging problems within the system, as has been observed numerous times in the Netherlands (van Beek,
128 2010). Therefore, detailed underground characterizations were used for the finalization of the pilot plants design and
129 monitoring in each site.

130 In particular, in order to obtain insight in the composition of the shallow subsurface and the quality of the groundwater,
131 geophysical well log measurements were performed at the Belgian and Dutch sites with a high resolution temperature
132 distribution multi tool, including:

- 133 - Gamma Ray (GR) measurement of the natural gamma radiation from the subsurface. Clay in general has a higher
134 gamma radiation than sand. For the GR-results the standardized unit gAPI (gamma-ray American Petroleum Industry)
135 is used. A high gAPI value indicates the presence of clay, a low value is an indication for sand, except when sand is
136 rich in clay minerals or in specific minerals such as Glauconite.
- 137 - Short Normal (SONO) measurement of electrical resistance (Ωm) in a specific zone (~0.5 m) around the tool. The
138 measured electrical resistance depends on the bore fluid, the diameter of the drilling, the groundwater and the
139 geological formation. Within an open hole with fresh groundwater, a relatively low electrical resistance indicates the

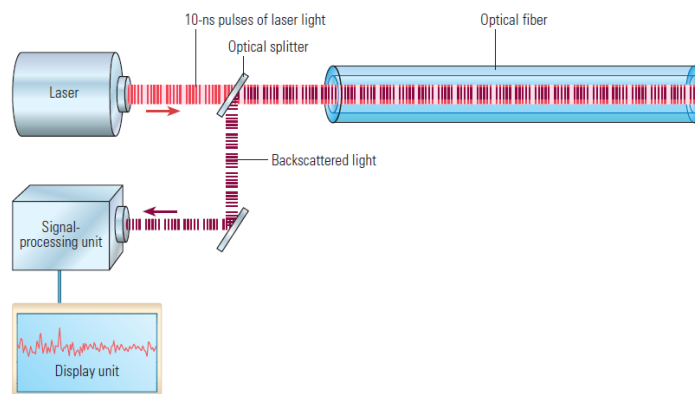
140 presence of clay and a relatively high electrical resistance is an indication of the presence of sand. In salt groundwater
141 the difference is not easily made.

142 - Long Normal (LONO) measurement, which is based on the same principle as the SONO measurement, but with a
143 larger range (~1.5 m), allowing more insight into the geological formation.

144 - Single Point Resistivity (SPR) measurement of the electrical resistance between the tool and a reference electrode
145 near the well is measured. The results can only be used qualitatively.

146 Distributed Temperature Sensing (DTS) was performed with a fibre optics device (see Figure 3).

147



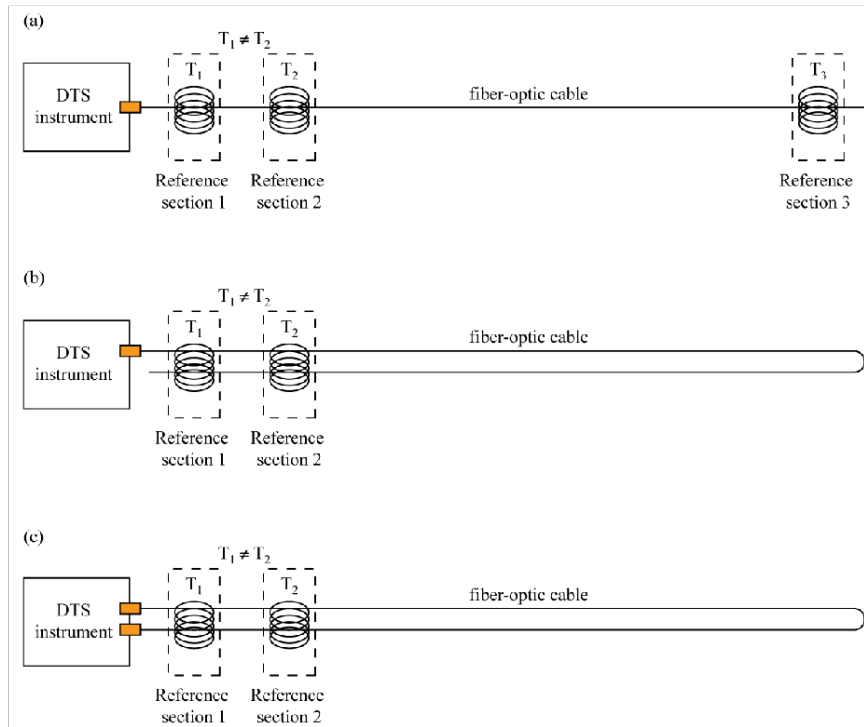
148

149 Figure 3. Temperature monitoring with fibre optics using raman backscatter DTS sensing.

150

151 Due to the harsh environment in the soil, data were collected in a single ended measurement manner using a double ended
152 setup (see Figure 4). Thus, both available channels can be used to correct for attenuation within the cable and temperature
153 offset. When a cable is damaged during the measurement period the double ended configuration setup doesn't work and
154 for the whole cable the data would become worthless. Hence, both sides were measured but stored in a single ended
155 configuration (see Figure 4b from Hausner et al, 2011). In this set-up it is possible to calibrate the single ended
156 measurements afterwards, so that a higher accuracy of the measurements is achieved.

157



158

159 Figure 4. Experimental measurement set-ups (Hausner et al., 2011) a) Simple single-ended configuration; b) Duplexed single-ended
 160 configuration; c) Double-ended configuration.

161

162 For each position on the fibre optic cable it is possible to define an x, y, z position. With these positions it is possible to
 163 process the fiber optic data into temperature distribution profiles, which form the basis for 3-d visualisation. A commonly
 164 used setup is that the fibres are installed in the subsurface around ATEs wells. At each position the fibres are connected
 165 to each other, so all positions can be monitored using only one channel connection.

166

167 **2.2 ATEs design for integration in smart district energy grid**

168 The combination of ATEs systems with district heating and cooling (DHC) networks has been obstructed by various
 169 techno-economic limitations: cooling networks hardly exist (Werner, 2017), high temperature networks complicate the
 170 use of sustainable sources of heat and the use of heat pumps (Kontu et al., 2019), and, finally, the economic model with
 171 cogeneration of power cannot be applied. In the last years a novel concept of DH network - the 4th district heating
 172 generation, also called “Low Temperature District Heating” (LTDH) - has been proposed (Lund et al., 2014), based on
 173 the following characteristics: i) to supply low-temperature thermal energy to new and existing customers, ii) to minimize
 174 thermal losses, iii) to integrate low enthalpy heat and iv) to become part of smart energy systems contributing to the
 175 transition towards a 100% renewable energy supply system characterized by the integration of different energy sectors.
 176 The LTDH definition identifies a wide range of temperatures: for example, a preliminary classification is proposed in

177 Averfalk et al. 2017 where “warm LTDH” and “cold LTDH” systems are distinguished based on the necessity to locally
178 boost the temperature at customer level.

179 Even if relevant barriers are still present in the development of LTDH systems (Pellegrini et al., 2019b), the combination
180 of ATES and low temperature DHC system is a promising solution for the implementation of a carbon-free heating and
181 cooling strategy. In fact, ATES systems can play a relevant role in the following fundamental topics related to existing or
182 new DHC systems:

- 183 - Increasing the efficiency of existing DHC networks: In the last few years, the selling price of power dramatically
184 dropped, and so the CHP business model is not sustainable anymore for DH networks. Since the use of reversible heat
185 pumps enables self-consumption of at least a part of the power produced by CHP plant, ATES systems can be seen as
186 a way to free the economics of DHC networks from the power selling price, and to increase the renewable energy
187 share.
- 188 - Seasonal storage: ATES systems can represent a key element in the seasonal efficiency increase of DHC networks,
189 since ATES systems are able to store excess heat in the groundwater in summer to be used in winter, and to store
190 excess cold in winter to be used in summer, that would otherwise be lost. ATES systems can be coupled with other
191 renewable sources (e.g. solar) and can add flexibility to both existing and new DHC networks.
- 192 - Decentralized heating and cooling production: ATES systems can be used in low temperature DHC networks as a
193 local and decentralized temperature booster or as a sink. So, ATES systems can balance temperatures of the cold
194 distribution network, thus favoring effectiveness and efficiency of the whole network. Moreover, ATES systems can
195 be used as decentralized heat/cold storage network elements.
- 196 - Power-to-heat and power-to-cool: reversible heat pump installation in DHC systems is a fundamental part in the design
197 of a smart energy grid, i.e. a multi-source grid integrating power grids, natural gas grids and DHC networks.
198 Converting electricity into heat (power-to-heat) or cold water (power-to-cool) through reversible heat pumps provides
199 flexibility for the electricity system, since operation is possible when electricity prices are low and/or when an excess
200 of electricity is produced by renewable sources (i.e. photovoltaics and wind turbines). When the ATES concept is
201 applied for power-to-heat and power-to-cool, there is the further benefit of using renewable energy as heat source or
202 heat sink and of allowing the storage of the heat and cold produced.

203 However, expertise and concrete projects in the field are limited and there is currently a lack of reliable and adequate
204 analytical tools and cost data to assess the technical-economic potential of ATES in combination with DHC networks
205 (Schmidt et al. 2018). The E-USE(aq) Italian pilot tried to overcome these barriers, since it combined a recirculating
206 ATES system with a cold low temperature DHC network.

207

208 **2.3 ATES energy performance monitoring**

209 Design and execution of the E-Use pilots were described in Pellegrini et al., 2019a with most relevant specifics, including
210 site maps, in the supplementary material. Detailed descriptions can also be found in Hoekstra and Van Gelderen, 2019
211 (project website). Methods and materials for pilot plants operation, measurements and monitoring of energy balances
212 were used in such a wide variety at the different pilots that they cannot all be described specifically within the limitations
213 of this paper. Since only commonly used and as far as possible certified methods and instruments were applied, these
214 details are not deemed relevant to the scope of this paper.

215

216 **2.4 Impact assessment of ATES in combination with bioremediation on groundwater quality**

217 In the Dutch pilot in Utrecht, complete Vinyl Chloride (VC) degradation was obtained within one day after bio-
218 augmentation of a chlorinated solvent reducing bacterial culture, measured at the bio-augmentation well, which was
219 situated approximately 5 m from the ATES well. Within a week, 90% contaminant reduction was also observed at the
220 monitoring well, situated approximately another 5 m downstream. Although this large effect was only temporary, as
221 shown in Pellegrini et al., 2019a, a year after bio-augmentation, a clear effect could still be observed. VC concentrations
222 in the ATES well fluctuate over the season, but there also appears to be an unexpected distinct decrease in the ATES
223 wells, 5 m upstream from the bio-augmentation well (Pellegrini et al., 2019a). Supposedly dechlorinating micro-
224 organisms, found in the ATES wells, have most likely migrated upstream – in line with the interference between hot and
225 cold layers shown in § 3.1 – via the cold well, to which deeper groundwater flows in the opposite direction, thus increasing
226 the proliferation of degrading organisms via the ATES system. Pellegrini et al., 2019a also shows that in the bio-
227 augmentation well, dechlorinating micro-organisms are still present one year after bio-augmentation. This provides
228 evidence that the observed long lasting VC reduction is indeed caused by continued degradation, although this could not
229 be proven by the presence of degradation products due to the low concentrations.

230

231 **2.5 Economic data and assumptions**

232 A crucial driver for increasing the Europe-wide implementation of ATES systems is demonstration of economically
233 feasible systems. Through the analysis of the pilot plants realized in the E-USE(aq) time framework it has been possible
234 to collect relevant data in different EU countries about the costs related to the design and installation, and operation and
235 monitoring of different ATES system combined with several technologies. Pilot plants have been operational from a
236 minimum of one to a max of four years.

237

238 **2.5.1 ATES systems for heating and cooling purpose**

239 Table 2 summarizes the relevant data used for the economic assessment of the different E-USE(aq) pilot plants
 240 characterized by heating and cooling purposes. The presented data have been used to feed an Excel sheet designed by
 241 Nomisma Energia Srl which automatically calculates the discounted payback period (DPP) for each pilot. DPP represents
 242 the number of years necessary to break even on the investment, while accounting for the discounted value of money
 243 (Short et al., 1995). DPP has been identified as an effective economic parameter to compare the different pilots with
 244 respect to investment payback and risk. The formula for DPP computation is reported in Equation 1, wherein the
 245 discounted yearly profit or loss is computed (cumulative cash flow, CCC). Yearly CCC are discounted through the annual
 246 interest rate i . Energy savings data have been measured for Delft, Ham and Nules sites, while in the case of Bologna pilot
 247 the energy figures are based on estimation. A peculiarity of the Italian pilot is the absence of power costs, which is due to
 248 the fact that the pilot plant owner is also the company manager of the Italian electricity grid and that the pilot plant is
 249 located in an electric station. As a result, power consumption of the pilot plant is negligible and not accounted.
 250 Nevertheless, this very specific condition is economically balanced by the high capital costs, as discussed in the following
 251 sections.

252
 253 Table 2. Main economic figures of ATES pilot plants for heating and cooling purposes.

Parameter	Symbol	Delft	Ham	Bologna	Nules
Capital costs (€)	CAPEX	62,000	116,000	460,000	58,000
Specific capital costs (€/kW th peak)	-	886	178	2,875	532
Natural gas consumption without ATES (Sm ³ /year)	ER _{NG}	11,500	188,000	24,000	36,000
Electricity consumption without ATES (MWh/year)	ER _E	27	297	20	3
Natural gas consumption with ATES (Sm ³ /year)	EATES _{NG}	0	58,100	0	14,315
Electricity consumption with ATES (MWh/year)	EATES _E	19	492	102	64
Natural gas cost (€/Sm ³)	c _{NG}	0.55	0.53	0.96	0.70
Electricity cost (€/MWh)	c _E	170	94	0	141
Operation and Maintenance costs of ATES (€/year)	C _{O&M}	2,000	16,000	2,000	266
Other costs of ATES system (€/year)	C _{other}	1,000	0	2,500	2,500
Annual interest rate (%)	i	6	6	6	4
Amortization period (year)	n	10	10	10	10

Average tax rate (%)	t_R	26	34	26	21
Depreciation rate used for tax (%)	d_R	5	0	5	3
Fiscal leverage (%)	f_L	0	0	0	50
Rate of deductible interest (%)	r_{DI}	30	30	30	30
Yearly incentives (€/year)	In	0	0	4,116 for 7 years	4,152 for 5 years
Co-financing incentives (€)	Inc	0	0	0	0

254

255 $CCC = - CAPEX - OPEX + OR + LA + TD$ (Eq. 1)

256 CAPEX includes all the capital costs (design, authorization/permit procedure, preliminary tests, realization and
257 commissioning of the pilot plants). OPEX can be computed as in Equation 2:

258 $OPEX = C_{O\&M} + C_E - R_E + C_{other}$ (Eq. 2)

259 where CO&M is the annual operation and maintenance cost of the ATES plant, C_{other} are other costs (i.e. administration
260 and insurance costs) related to ATES system operation, C_E and R_E are computed as, respectively, yearly energy costs of
261 the ATES system in Equation 3 and yearly energy revenues or the energy savings produced by the ATES system if
262 compared with the reference situation (i.e. before ATES installation) in Equation 4.

263 $C_E = \sum c_i \cdot E_{ATES-i}$ (Eq. 3)

264 $R_E = \sum c_i \cdot E_{R-i}$ (Eq. 4)

265 OR includes other yearly revenues, that are yearly incentives In and co-financing incentives Inc. An example of yearly
266 incentives are the white certificates, while an example of co-financing incentives are regional, national and European co-
267 funds. LA is the loan amortization, while TD is the tax deduction.

268

269 **2.5.2 ATES in combination with bioremediation**

270 In cases where ATES can be combined with ground water remediation, a payback analysis of costs of energy or avoided
271 greenhouse gas emissions does not offer a complete picture. In these cases, the value of clean groundwater should also
272 be taken into account, which is hard to determine, and compared to standard remedial costs, which are evaluated in the
273 paper. Only rough estimates can be made for the total costs of a combined ATES + Bioremediation project, since the
274 frequency of bacterial batches to be grown and infiltrated into the soil per year is not yet known, because the long-term
275 durability of the bacterial mass is still unknown. Obviously, the number of batches will strongly influence the total costs.

276 For a rough estimation and comparison, a VOC contaminated groundwater volume of 100,000 m³ is imagined. The
 277 specific and discounted treatment cost per cubic meter of contaminated groundwater can be computed for different
 278 technologies starting from the data summarized in Table 3. Remediation technologies costs and performances are based
 279 on expert judgement and the Dutch soil quality recovery guidelines, 2019.

280

281 Table 3. Main economic figures of different state-of-the-art technologies used for groundwater remediation.

Parameter	1. Pump and treat	2. Bioaugmentation	3. Chemical oxidation
Contaminated volume (m ³)	100,000	100,000	100,000
Treated volume (m ³)	1,000,000	137,600	100,000
Specific treatment cost (€ per treated m ³)	1.50	3.85	35.00
Treatment duration (year)	11.5	2	1
Annual interest rate (%)	1.5	1.5	1.5

282

283 For case 1, using traditional groundwater remediation technologies (i.e. pump and treat), normally ten times the
 284 contaminated volume must be pumped and treated to remove contaminants. For the hypothetical contaminated groundwater
 285 volume given above, the treatment of 1,000,000 m³ will be necessary, with an average price of € 1.50 per m³ (including
 286 often needed additional iron removal). The time required for the completion of the treatment is estimated as 11.5 years,
 287 based on a 10 m³/h of flow.

288 In case 2, bioaugmentation technology is applied (like TCE/BEAT®) and low-density bacterial culture cultivated on-site
 289 are injected into the groundwater. The treated water is 1.4 times contaminated groundwater volume, with a specific
 290 treatment cost of about 3.85 €/m³. Here, the required time to complete the treatment can be estimated at about 2 years.
 291 Finally, in case 3, groundwater remediation with chemical oxidation, e.g. with (per)ozone, would require one year against
 292 approximately € 3,500,000 of remediation cost, being € 35/m³.

293 For ATES and bioremediation the calculations are based on a treatment period of 25 years in a new or existing ATES
 294 system, resulting in 50 cycles of groundwater flow through the activated zones and one batch of 10 m³ of bacterial culture
 295 per year in order to obtain sufficient degradation capacity. In total 25 batches of biomass injection are necessary. It is
 296 possible to assume a cost of approximately € 40,000 or € 20,000 per batch in the case of, respectively, limited or wide
 297 market up-take of the technology.

298

299 **2.6 Climate impact of ATEs systems**

300 In the Netherlands, where ATEs is more common, the registrations of ATEs systems and the national CO₂ emission
301 reduction accounting indicate that the average greenhouse gas (GHG) emission reduction per ATEs-system is between
302 45 and 80 ton CO₂/year (originally derived from CBS, 2009, and van Agt, 2011), strongly depending on reference case,
303 size, type of building and climate. On the basis of energy savings reported in Table 2, it has been possible to compute or
304 estimate the equivalent CO₂ emission reduction produced by the ATEs systems in each pilot. Equivalent CO₂ emission
305 related to power consumptions have been computed by considering the mean efficiency of the thermoelectric plants for
306 each country (see Table 4).

307

308 Table 4. Conversion factor of kg of CO₂ equivalent per Sm³ of natural gas burned and MWh of electric power produced
309 (Koffi et al., 2017).

Parameter	Value	
CO ₂ emission from natural gas combustion (kg CO ₂ /Sm ³ of natural gas)	1.87	
CO ₂ equivalent emission per power production (kg CO ₂ /MWh el)	342	ITA
	247	SPA
	451	NED
	196	BEL

310

311 **3. Discussion**

312 The chapter provides an interpretation of the main findings of the E-USE(aq) project by focusing in particular on how the
313 integration of ATEs with different renewables and renewable-based technologies can produce economic benefits as well
314 as positive impacts on the environment.

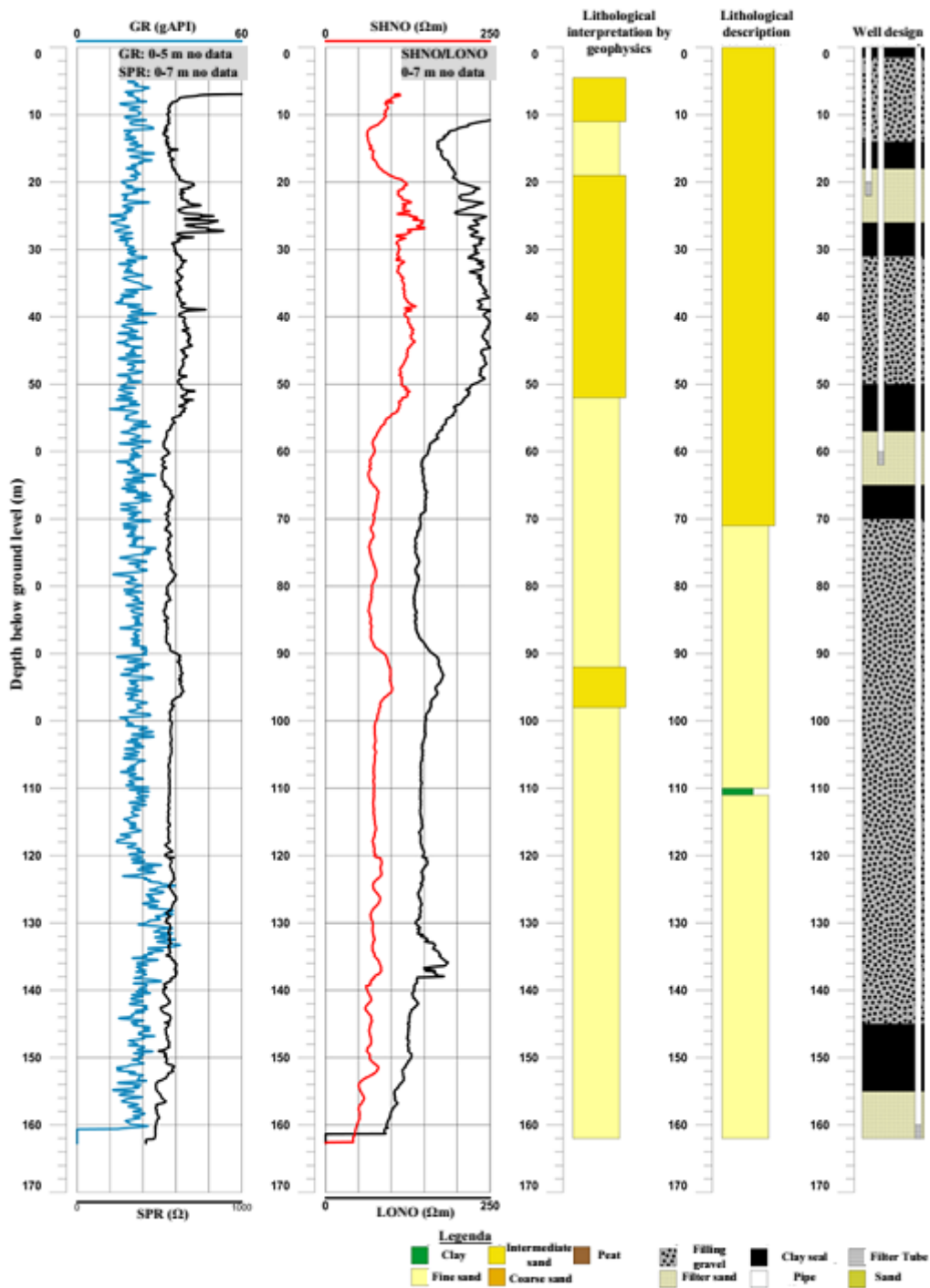
315

316 **3.1 Subsurface monitoring results**

317 **3.1.1 Belgian site**

318 Results of state-of-the-art monitoring technology used for the Belgian pilot are shown in Figure 5. A combination of
319 geophysical measurements and expert judgement generates an interpretation of the soil profile based on which a basic
320 extraction/infiltration and monitoring well design configuration was suggested. However, at the time the wells of the
321 ATEs system had already been installed without characterization of the deep subsoil. During installation, it turned out
322 that the aquifer was much deeper than expected, which provided the opportunity of installing considerably longer well

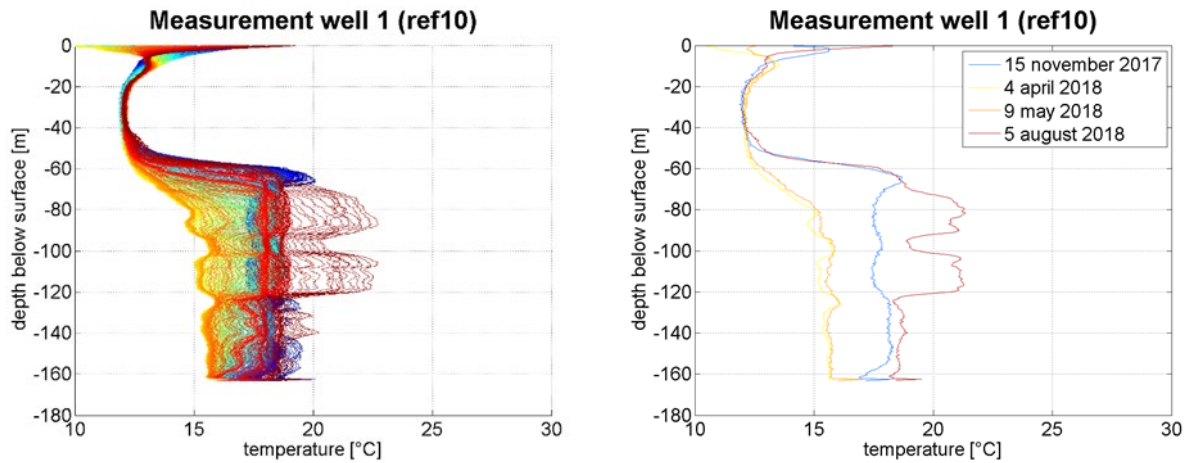
323 screens than originally planned, resulting in increased system capacity and a higher energy yield. In this case, it was
 324 possible to change the planned design quickly, otherwise this opportunity to increase capacity would have been missed.
 325



326
 327 Figure 5. Illustration of combined geophysical measurements resulting in a soil profile and a well design. GR=Gamma Radiation;
 328 SPR=Single Point Resistance; SHNO=Short Normal; LONO=Long normal.
 329

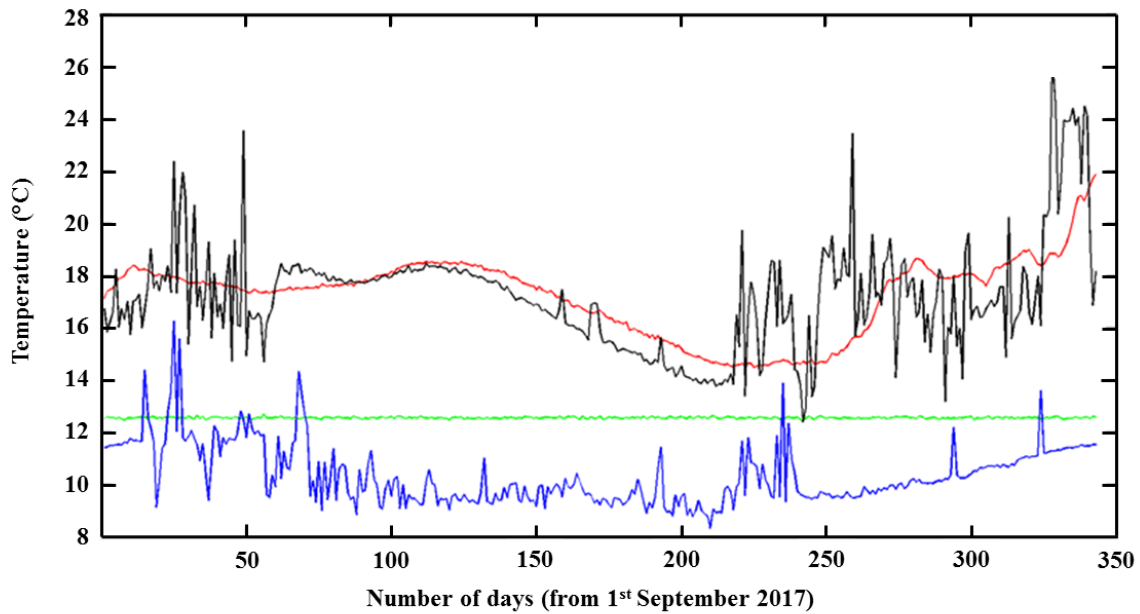
330 At the Belgian pilot, high resolution soil temperature distribution measurements were performed. The evolution of
 331 increased temperatures in the hot well and low temperatures in the cold well are illustrated in Figure 6, which shows the
 15

332 vertical temperature distribution in measurement well 1, at 10 m downstream from the hot well. In this figure, temperature
333 differences probably related to permeability differences can be observed within the aquifer, with lower permeabilities
334 around 90 m – bsl and the lowest 40 m of the well screen. In the layers with the highest permeabilities, the sphere of
335 influence will be the largest. The continuation of temperature monitoring could provide an early warning for possible
336 development of clogging pinpointed at specific depths in the filter.
337



338
339 Figure 6. Temperature distribution in the monitoring well, 10m away from the warm well (01/10/2017 – 30/09/2018) in Ham (Belgium).
340 Colors change gradually over time, starting with blue in September 2017 and ending with red in August 2018. Well screen is located
341 between 80 – 160 m bsl.

342
343 Monitoring well 2, situated downstream between the two ATES wells, showed no sign of interference between the hot
344 and the cold well (see Figure 7). This provides important information in assessing possibilities for implementation of
345 additional ATES wells and / or systems in the proximity of the installed plant.
346



347 **Monitoring well #1** **Monitoring well #2** **Monitoring well #3** **Monitoring well #4**

348 Figure 7. Temperature evolution in days after 1 September 2017 (day zero) at 80m depth for the 4 different wells in Ham. Monitoring
 349 well 1 is situated at 10 m downstream from the hot well (production well 1). Monitoring well 2 is situated further downstream between
 350 the hot and the cold well.

351

352 3.1.2 Spanish site

353 At the Spanish site, with a detrital multilayer aquifer of variable thickness from 50 to 270 m, in situ tests to determine
 354 flow velocity and permeability were carried out to define the best position of the monowell filters that would ensure
 355 minimal impact on aquifer properties in line with Spanish regulations for which it was specifically adapted (as described
 356 in Pellegrini et al., 2019a), resulting in a system that is also very suitable for thin aquifers.

357

358 3.1.3 Italian site

359 At the Italian site, only a small water bearing layer of (< 10 m) was found. The ambient groundwater flow was measured
 360 with a pumping and a tracer test (see Hoekstra and Van Gelderen, 2019; Conti et al., 2019) and found to be about 80-100
 361 m/year, which is considerably higher than 25 m/year, that is considered as an upper limit for conventional ATEs systems.
 362 Therefore, only a recirculation system (see Figure 1) was deemed possible at this site.

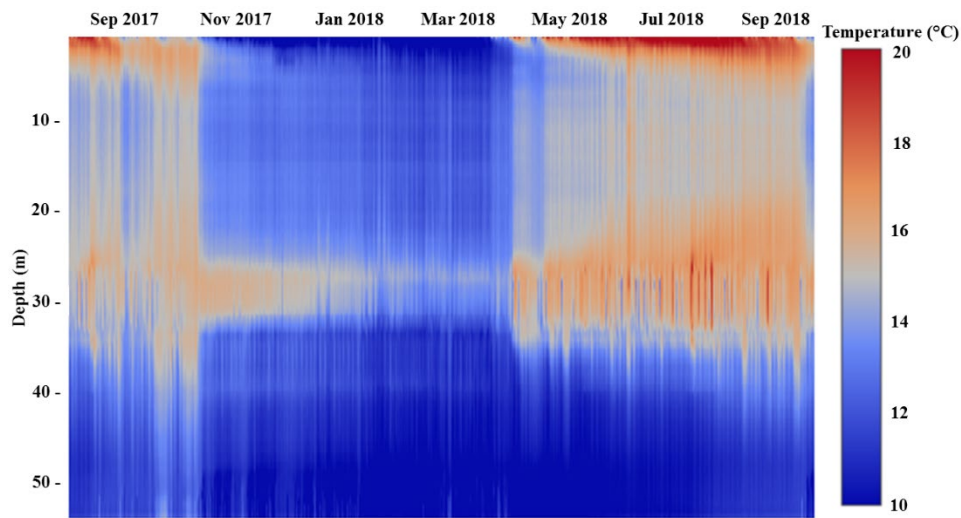
363

364 3.1.4 Dutch sites

365 In both Dutch pilots in Delft and Utrecht, high resolution soil temperature distribution measurements were performed. In
 366 the Utrecht monowell system probable interference between hot and cold layers could be observed, as illustrated in Figure
 367 8. Figure 8 shows that at certain time intervals in summer a warm zone extends vertically into the cold zone, most probably

368 caused by the absence of an aquitard. Data suggest that the injection of warm water during summer has a ‘downward
369 influence’, which is in contrast with the initial assumptions and modelling.

370



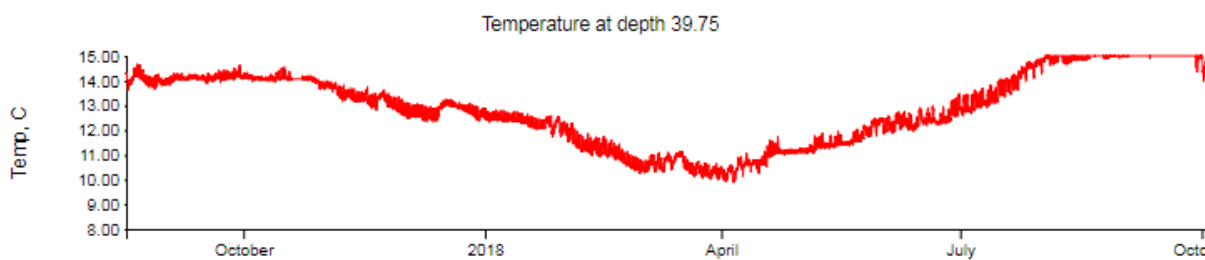
371

372 Figure 8. Temperature distribution in monowell (ATES-3) from September 2017 to October 2018. Scale bar (right) shows temperature
373 range in °C. The positions of the warm (26 – 31 m bsl) well and cold well (49 – 56 m bsl) can be seen.

374

375 Figure 9 shows the temperature profile recorded in the middle well screen of the monitoring well, and from this it can be
376 observed that the warm water also extends to this depth at the monitoring well (situated about 10 m from the ATES well),
377 as temperatures are around 14-15°C during the summer period and decrease to 10°C in the winter period.

378



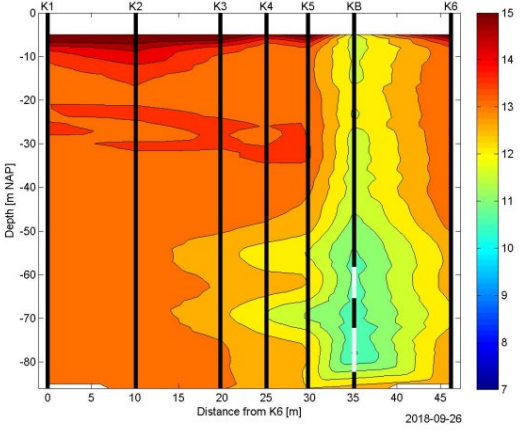
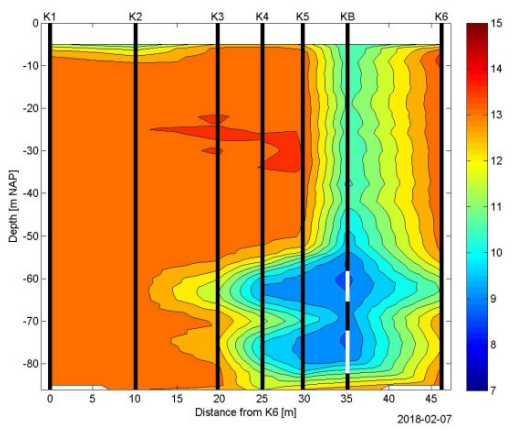
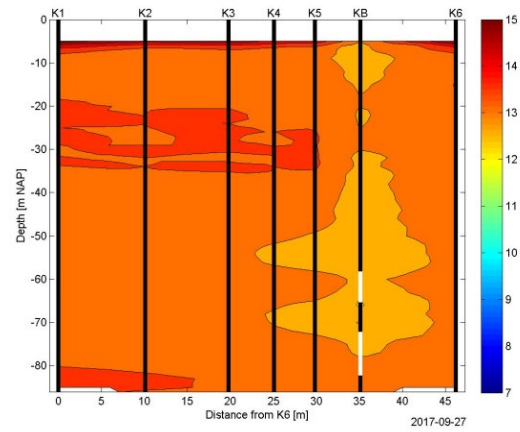
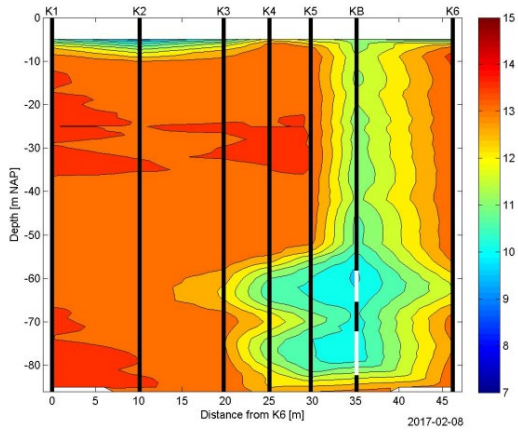
379

380 Figure 9. Temperature profile at the middle filter of the monitoring well (40 m). ‘2018’ on the horizontal time axis marks January 2018.

381

382 Figure 10 presents spatial images of the temperature distribution around the cold well in Delft (Netherlands) at the peak
383 of the heating season and at the end of the cooling season in 2017 and 2018. In the first year, it can be observed that there
384 is less cold stored in the underground during winter, and that the cold reservoir is completely depleted at the end of the
385 summer. In the following year, both climate conditions and operational system optimizations (Pellegrini et al., 2019a)
386 allowed the storage of more cold, which was sufficient for the cooling demand.

387



388

389

390 Figure 10. Spatial temperature measurements in Delft (Netherlands), derived from high resolution measurements in glass fiber cable
 391 at 6 distances around the cold well.

392

393 **3.1.5 Danish site**

394 The geology consists of a thin layer of fill. A layer consisting of sandy moraine clay to a depth of approximately 14 m
 395 bgl (+40 m above sea level) is found beneath the layer of fill. Under the layer of moraine clay, glacial melt water sand
 396 deposits are found with a total thickness of 44 m. The sand varies between coarse, medium and fine-grained sand in the
 397 top 24 m of the layer followed by 20 m of fine well sorted sand. Below the massive sand layer, the surface of the chalk is
 398 encountered, approximately 60 m bgl. The primary aquifer in the area is connected to the chalk and the overlying glacial
 399 melt water sand deposits, with an unconfined water table. There is a direct hydraulic connection between the glacial melt
 400 water sand deposits and the chalk in the area. There is no secondary aquifer. The water table is found about 21 m bgl. The
 401 top 3 m of the aquifer is described as brown/oxidized and below this the sediment changes color to grey and the conditions
 402 are anoxic.

403

404 3.2 ATES combination with district heating and cooling networks and smart grids

405 The Italian pilot plant concept has been developed to be highly replicable, including at a larger scale, with the aim of
406 demonstrating the benefits of ATES and DHC integration on an operational electrical station. The plant consists of three
407 extraction and three injection wells (plus four monitoring wells) that feed via a secondary circuit three reversible open-
408 loop heat pumps, each one of about 70 kW_{th}, and one open-loop chiller with a nominal cooling capacity of about 55 kW_{th}
409 (see Conti et al., 2019). The ATES pilot plant delivers thermal energy to two buildings located in an electric station near
410 Bologna. One building includes also data centre rooms which need cooling throughout the year. Figure 11 shows a
411 schematic of the Italian pilot plant. The novelty of the pilot plant design lies in the fact that the energy distribution system
412 is a cold low temperature DHC network fed by the ATES system. Two substations (one for each building) are present.
413 The geothermal energy source acts as the centralized heating/cooling unit, while the space heating and cooling demand
414 is covered by the operation of the local reversible heat pumps or chillers. The secondary circuit works as a compensation
415 element that is kept at an optimized temperature. In summertime all the substations work to produce cold water for space
416 cooling. The secondary circuit has been designed to work at approximatively 20 °C, while the cold water is stored in the
417 substations at 10-12 °C. In wintertime, warm and cold water need to be produced at the same time to satisfy both the
418 demand for space heating and space cooling, the latter coming from the data center rooms. When the heat extracted from
419 the secondary circuit for space heating exceeds the heat sunk in the secondary circuit for data center rooms cooling, the
420 temperature of the secondary circuit decreases and is heated up by the geothermal source. In this case, the cold water tank
421 is cooled down without using the chiller, but through a heat exchange with the secondary circuit. Conversely, when the
422 heat taken from the secondary circuit for space heating is about the same or lower than the heat sunk in the secondary
423 circuit for data center rooms cooling, the temperature of the secondary circuit would increase, and the chiller is put in
424 operation to guarantee the data center rooms cooling. In this condition, the waste heat coming from the data centers is
425 recycled via the heat pumps for space heating, and the geothermal source has limited or no contribution on the system.
426 Therefore, the Italian pilot aims to demonstrate how the recycling of waste heat in a cold low temperature DHC network
427 can be practically realized and how renewable energy sources, ATES in particular, can be used to compensate the
428 mismatch between heating and cooling demand, if present. The ATES system aims to substitute the existing natural gas
429 boilers and water-to-air chillers. Nevertheless, the ATES pilot plant is integrated with the existing water-to-air chiller and
430 two electric boilers of 57 kW_{th} each (one for each building), which are connected to the water tanks and can be used as
431 back-up unit of the ATES system for space heating or cooling.

432

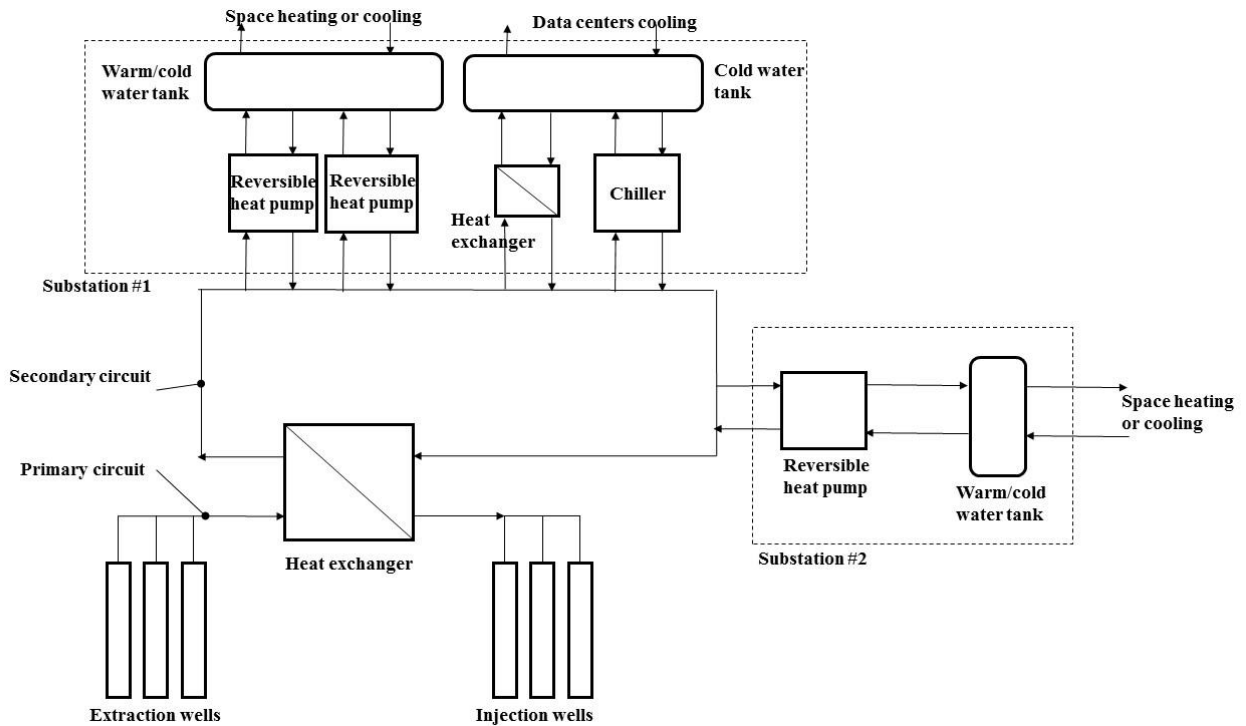


Figure 11. Schematic of the Italian pilot plant.

433

434

435

436 3.3 Combination with solar heat collection and photovoltaic electricity generation

437 The combination of ATEs with solar energy production was tested in both the Belgian pilot and the Dutch pilot in Delft.

438 In Ham in Belgium a state-of-the-art PVT-system was used (35 BLO-260 TripleSolar PVT-panels placed on the roof of

439 the office building, accounting for 119 m² of PVT surface and 18,2 kW of peak power production) that allows for more

440 electrical output at high ambient temperatures than conventional PV-cells, by removing excess heat, thus avoiding the

441 normally observed output decrease with temperature increase. The conveyed heat can be used to generate domestic hot

442 water, but excess summer heat can also be stored in the subsoil via the ATEs system and applied usefully in winter. It is

443 also possible to use the PVT-panels to generate additional cooling capacity for use in summertime. The annual energy

444 that can be charged/discharged strongly depends on the entering fluid temperature. Water coming from the Belgian ATEs

445 is about 10°C to 13°C. At 10°C entering fluid temperature about 3000 MJ/m²/year heat can be charged or 1100 MJ/m²/year

446 of heat can be discharged according to the technical documentation of the panels. Although relatively small, the PVT-

447 systems provide means to balance the ATEs in two directions. Due to an error in the electricity sensor of the PVT panels,

448 data is only available until June 2018. For this reason, the performance of the PVT system is evaluated for the period

449 January 2018- June 2018. In this period the measured electricity production was 9,117 MWh while the warm water

450 production measured 5,831 MWh. Since the yearly design output values are 18,636 MWh electrical and 10,383 MWh

451 thermal, performance was in line with expectations.

452

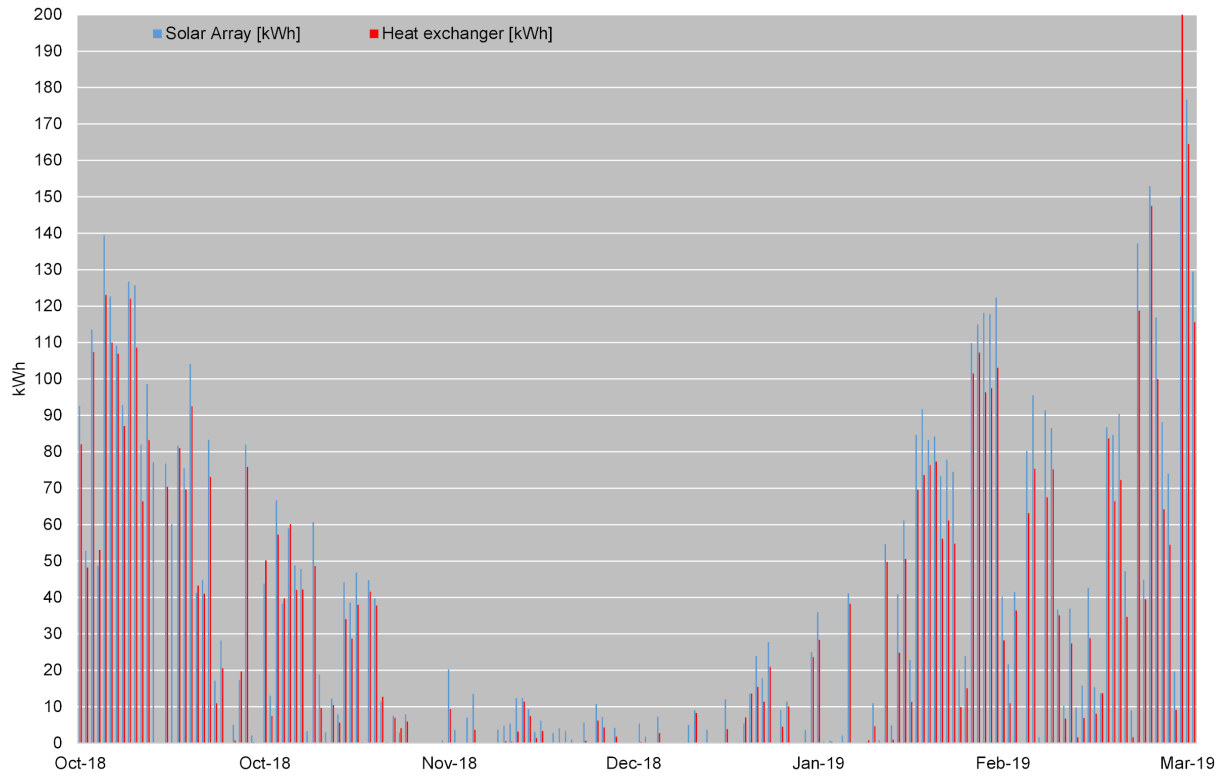
453 In Delft in the Netherlands an innovative Virtu solar system was integrated and tested. This system can generate more
454 thermal output than flat panel PVT collectors in cool climates, since it includes a vacuum tube that reduces thermal losses.
455 Installation was carried out in two phases, firstly a pilot system of just 10 tubes and then, towards the end of the project
456 period, a larger installation of 120 tubes. This new array was operated for six months, generating the data shown in Figure
457 12 and Figure 13. However, the increased heat generation (combined with cooling loads from the buildings) resulted in
458 the aquifer temperature increasing above planned control limits. Therefore, in April 2019 the Virtu solar array had to be
459 covered, since the heat could not be dissipated within the climate-control system.

460

461 Based on the phase 1 data from the small test system of 10 tubes, it was decided to secure frost prevention by connecting
462 the phase 2 array of 120 PVT tubes to the ATES-system via a heat exchanger. The heat exchanger was connected to the
463 cold well output side of the ATES system. A second connection, between the solar array and the warm well is now being
464 considered, as this would allow more flexible use or storage of heat as a function of season. These operational issues
465 provided valuable practical experience of solar array integration with an ATES system, but the delays and over-heating
466 issues have meant that it has not yet been possible to measure temperature distribution effects in the soil following the
467 phase 2 solar array installation.

468

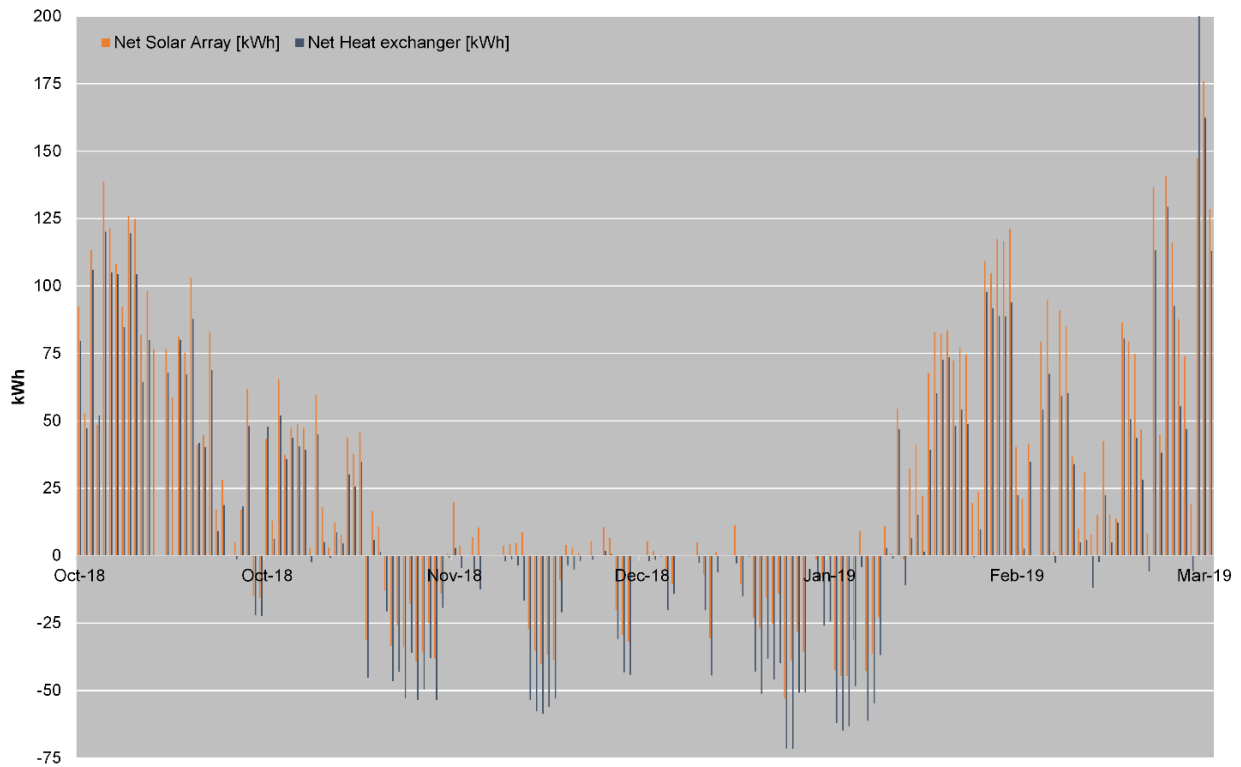
469 Figures 12 and 13 show the Virtu solar array production in Autumn 2018 and Winter 2019. Heat production is good in
470 October and February/March with an output of >100 kWh per day on sunny days. Figure 12 shows the daily “positive
471 energy”, excluding heat losses. Excluded from this data are any periods where the measured power was negative, such as
472 on cold cloudy days or frosty nights. Based on this dataset, the total heat energy measured in the period October 2018 to
473 March 2019 was 6.5 MWh of heat generated (measured at the solar array), with 5.7 MWh of this delivered to the heat
474 exchanger. This shows that, on good solar generation days, the efficiency of the pipe-work and heat exchanger system
475 was good in collecting and transferring heat. Figure 13 charts data from the same period, but in this case including the
476 periods of heat loss (i.e. when measured heat is negative). For this “net energy” data set the total heat energies were 4.8
477 MWh generated and 2.7 MWh delivered.



478

479 Figure 12. Measured “positive energy” in Delft: generated heat, with energy losses excluded. The figure includes 2 data sets: the array
 480 energy and the heat exchanger energy. The array energy is from temperatures sensors at the array and shows the energy generated by
 481 the Virtu collectors. The heat exchanger is from temperature sensors in the plant room and shows how much was delivered to the
 482 system. The fact that these 2 data sets match quite closely shows that heat losses from the pipework and system are quite low.

483



484

485 Figure 13. The measured “net energy” in Delft (like in Figure 12, measured at the thermal array and at the heat exchanger) which
 486 integrates the power over 24 hours and includes the frost-prevention approach of circulating water at night, so the figure shows the true
 487 total energy delivered by the PVT-system to the ATES / climate control system.

488

489 The large difference between the “positive energy” and the “net energy” totals is caused by the frost prevention method
 490 used in the system, which involved losses due to continuous water circulation through the tubes at night whenever ambient
 491 temperature fell below 5 °C (using circulating water temperature of 20 to 30 °C). It is noted that freezing prevention could
 492 be realized with much lower power, using water at lower temperature and flow rate, or through use of glycol solution
 493 instead of water (in which case no circulation would be required). During this period of the project, heat loss reduction
 494 was not a priority. Longer term, energy output will need to be balanced throughout the annual cycle and reduction of this
 495 night time loss can form part of the improved integration between the PVT solar array and ATES system. However, this
 496 illustrates that the Virtu solar array can also be used in a night-time cooling capacity, which could be applicable to warmer
 497 locations, although flat plate PVT systems would be more suitable for that goal.

498

499 The thermal power output demonstrated by Virtu in February 2019 shows the advantage of vacuum tube thermal
 500 insulation for solar heat production in cool climates. The target temperature for heat production from the array was 40-45
 501 °C and efficient thermal power levels, above 20 kW, were achieved at this temperature on sunny days during

502 February/March 2019, even when air temperature was below 10 °C. The reduced heat loss to the ambient with the vacuum
503 tube technology (compared to flat panel solar thermal and PVT collectors such as used in the Belgian pilot) also enables
504 higher temperatures and thermal powers during spring and autumn and is therefore of particular relevance to solar thermal
505 ATES installations in cool climates. The Virtu collector is available in two versions: a hybrid PVT version and a thermal-
506 only HOT version. Other field installations of Virtu PVT in the UK have demonstrated similarly effective heat production
507 at low ambient temperature as at the Delft site. Independent testing of Virtu PVT carried out at the TUV Rheinland solar
508 test lab has demonstrated combined heat and power generation of 226 W per tube at 929 W/m² of solar radiation and a
509 medium water temperature of 32 °C above ambient temperature, which represents a total energy efficiency of 77% based
510 on absorber area or 57% based on aperture area. This is significantly higher efficiency than can be achieved by flat panel
511 PVT collectors operating in this temperature range (Mellor et al., 2018).

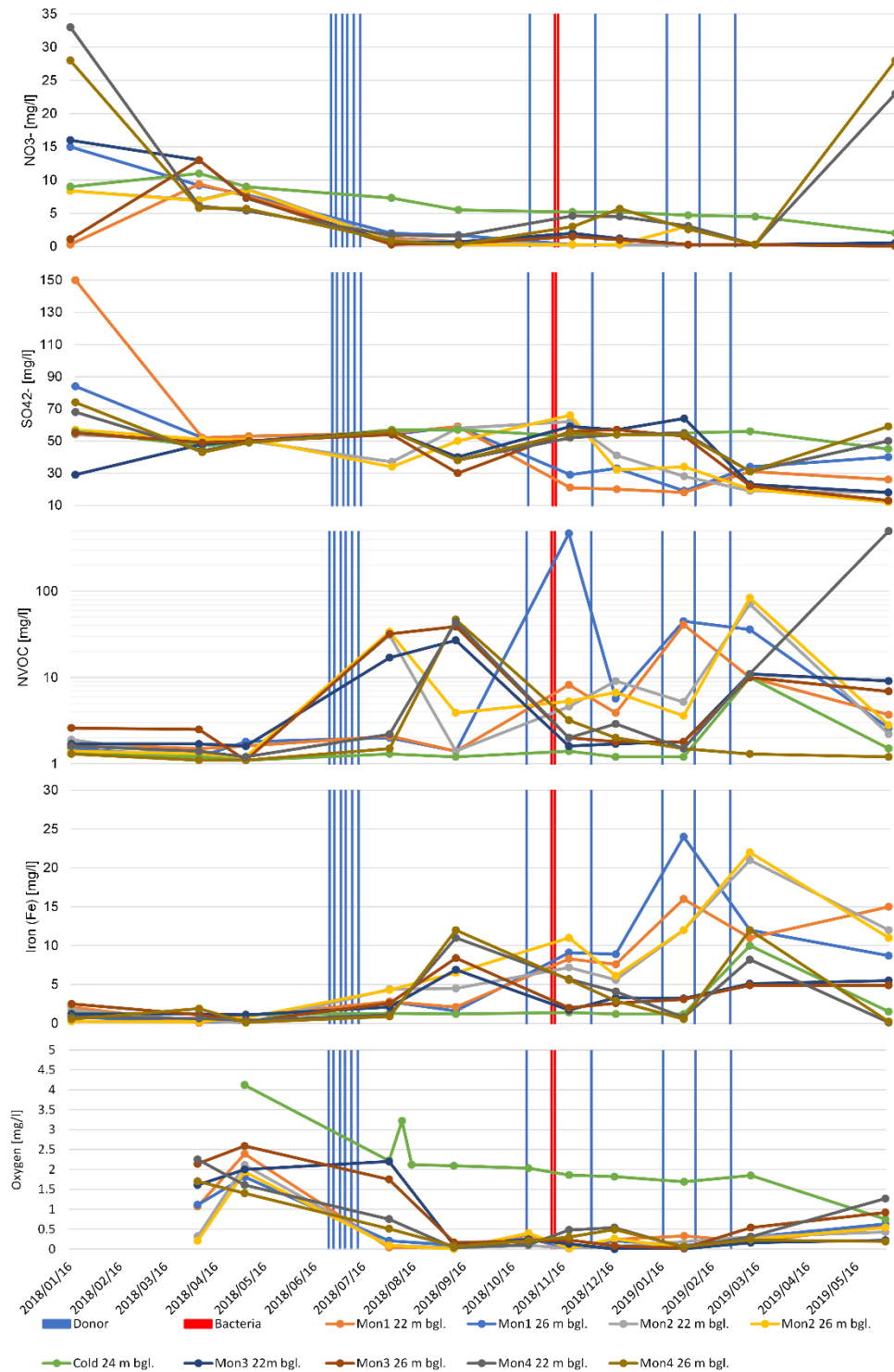
512

513 **3.4 ATES in combination with bioremediation: new experimental results about groundwater** 514 **quality assessment**

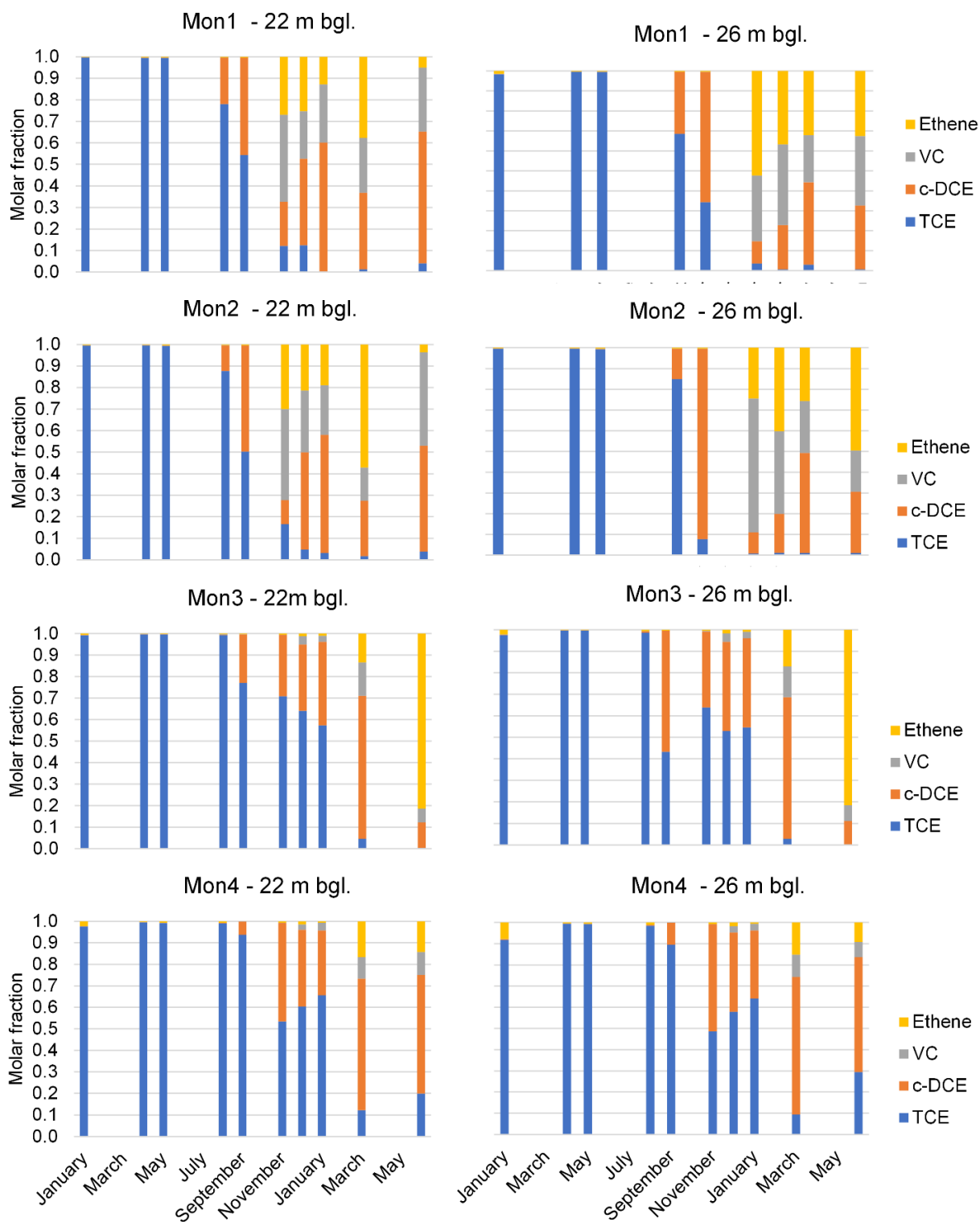
515 At the Dutch pilot site in Utrecht samples were taken on 17 September 2019, more than a year after the last monitoring
516 round, as published in Pellegrini et al., 2019a, in order to test the long-term longevity of the performed bio-augmentation.
517 In soil mesocosms in monitoring wells downstream from the bio-augmentation well still high concentrations of
518 dechlorinating bacteria were found: $2,0 \times 10^6$ (in screen 38-42 m bgs) and $6,7 \times 10^5$ (in screen 53-57 bgs) and in the
519 groundwater in the $3,4 \times 10^4$ *Dehalococcoides bacteria* cells; with about 1/3 of the latter detected to be viable. Concordant
520 with these results, almost no VC was detected in most of these wells anymore. The maximum VC concentration was 0.3
521 µg/l, found in the upper ATES well (27-32 m bgs), while preceding bio-augmentation these wells contained 2.4 – 4.3 µg/l
522 VC. It appears that both bio-augmentation longevity and radius of influence – enhanced by ATES operation with induced
523 seasonally reversing groundwater flows – is even much larger than expected.

524 While at the Dutch pilot site in Utrecht only low plume zone concentrations of VC were present in iron to sulfate reducing
525 redox conditions, the Danish pilot site had high concentrations of trichloroethylene (TCE) in an aquifer with oxidative
526 conditions hostile to organisms capable of reductive dichlorination. The deeper part of the aquifer was chemically
527 reduced. Bench testing showed that electron donor injections could not be avoided, with consequently there was an
528 imminent risk of clogging. Since the recirculation system was only used for testing purposes, with no need for utilization
529 of the energy produced, the clogging risk was acceptable. However, clogging was effectively prevented by a filtration
530 unit between the extraction and infiltration filter. A total of 12,000 m³ of water was extracted, heated from 12°C to 20°C
531 and re-infiltrated, from March 2018 to March 2019. Figure 14 shows that with repeated electron donor (lactate and acetate)

532 additions, organic matter reached all monitoring wells and consequently electron acceptors were reduced, leading to low
 533 concentration of oxygen, nitrate and sulphate and high concentrations of reduced iron that dissolved from the soil.
 534



535
 536 Figure 14. Following electron donor additions into the hot well at the Danish site, organic matter (NVOC) and dissolved iron
 537 concentrations increase in all monitoring wells, while electron acceptors oxygen, nitrate and sulphate concentrations decrease.
 538 Monitoring wells 1,2, 3 and 4 are situated on a straight line between the hot and the cold well.



539

540

Figure 15. Degradation in monitoring wells at the Danish site as molar fraction of total contamination present.

541

542

Figure 15 shows that partial reductive dechlorination, to cis-dichloroethylene (c-DCE), started after the initial electron

543

donor injections in July 2018. Beginning of November 2018, conditions were deemed adequate for the cultivated

544

dehalogenic culture. After bio-augmentation in monitoring well 1 and 2, complete dechlorination to ethene was observed

545 in most monitoring wells, especially in the ones closest to the hot injection well. In the cold extraction well, only little
546 effect could be observed, owing to dilution by the surrounding groundwater.

547 From Utrecht and Copenhagen pilots it can be derived that ATES can both enhance soil remediation performance on
548 highly contaminated sites and accommodate groundwater quality improvement, as a tool in groundwater management
549 implementation.

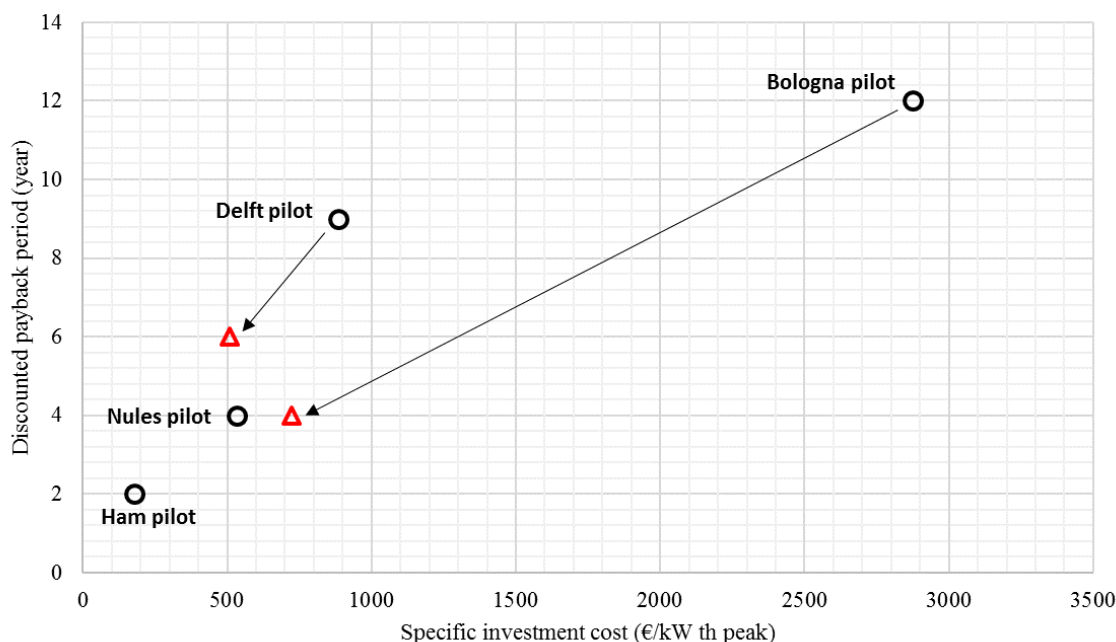
550

551 3.5 Economic assessment

552 3.5.1 Energy savings and related economic benefits

553 The black circles in Figure 16 show the DPPs calculated for four pilots accordingly to the data presented in Table 2. Since
554 economic conditions can vary widely locally and with time, these numbers only give a rough indication. Nevertheless,
555 the computed DPPs times are in the range from 2 to 12 years that are found on average for state of the art ATES systems
556 in the Netherlands, showing that the system innovations and innovative combinations demonstrated in the E-USE(aq)
557 project, in order to overcome barriers, do not hamper the economic feasibility of ATES. On the contrary, for the Belgian
558 and Spanish case significantly improved DPPs were achieved, reinforcing that ATES represents an economically
559 attractive technology. Nevertheless, in Figure 16 two further DPPs are presented with red triangles, that are the DPPs that
560 may be achieved by Bologna and Delft pilots under certain conditions.

561



562

563 Figure 16. Computed discounted payback periods (DPPs) for the E-USE(aq) project pilot plants.

564

565 For the Italian case study, the investment costs stand out as much higher than the other pilots. In fact, the Italian pilot
 566 plant is characterized by high redundancy, justified by the type of application (i.e. space heating and cooling of an electric
 567 station, wherein a high safety standard has to be satisfied, in particular for the data center rooms). Also, the framework
 568 conditions (revamping of the warm and cold water distributing system, realization of a new substation for one building
 569 served by the pilot plant, realization of a centralized and automatized control panel for the whole heating/cooling plant),
 570 and the monitoring requests made by the regional authority that issued the permits, increased the investment cost
 571 compared to the other plants. These elements make the Bologna pilot somewhat unique and not directly scalable (in terms
 572 of costs) to other similar applications, i.e. ATES in combination with DHC networks. For a generic commercial scale
 573 DHC network, the projected investment required would be 724 €/kWth (peak power), which would result in a DPP of
 574 about 4 years.

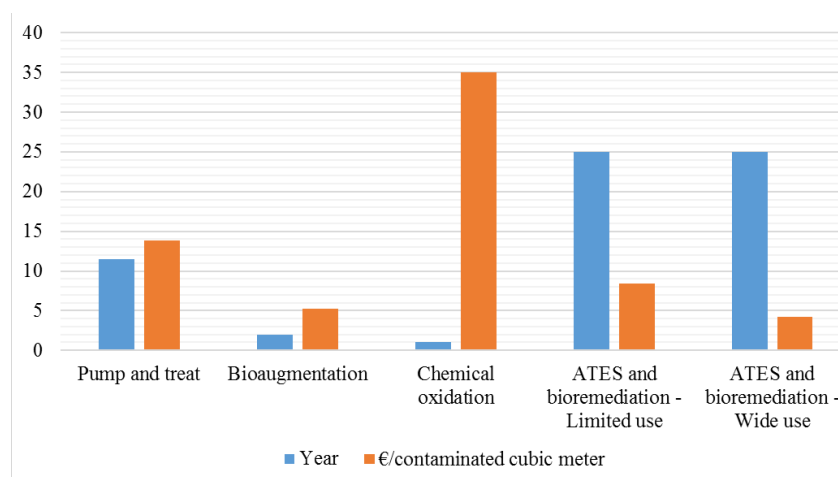
575 The DPP for the Delft pilot would also be reduced at scale, taking account of the relatively high cost of the 120 Virtu
 576 tubes. For a larger system of 1000 Virtu tubes, it has been projected that the reduced investment costs and increased
 577 energy savings would reduce the investment to 508 €/kW th peak, leading to a DPP of 6 years.

578

579 3.5.2 Economics of ATES in combination with bioremediation

580 The specific and discounted cost of groundwater treatment has been computed, starting from the information included in
 581 Chapter 2.5.2. The results of the comparison are shown in Figure 17. ATES and bioremediation can be competitive with
 582 the existing biological *in situ* treatment options and is much more cost efficient compared to traditional remediation (pump
 583 and treat) and chemical oxidation. A wider use of the technology could further increase the competitiveness of ATES
 584 with bioremediation compared to bioaugmentation alone.

585



586

587 Figure 17. Results of the economic comparison of different groundwater remediation technologies: treatment duration and discounted
 588 cost per cubic meter of contaminated groundwater for pump and treat, bioaugmentation, chemical oxidation and ATES+bioremediation.

589

590 A further advantage of the ATES with bioremediation approach is that ATES can start operations without the necessity
591 of remediating the groundwater first, which could take many years. In this respect, only chemical oxidation is a relevant
592 alternative technology, because only with this technique could sufficient groundwater remediation be reached within one
593 year, to allow installation of an ATES system into clean groundwater afterwards. However, chemical oxidation is 4-8
594 times costlier than ATES in combination with bioremediation. Moreover, chemical oxidation influences the groundwater
595 geochemical composition and results in decreased suitability for ATES. So, compatibility of chemical oxidation and
596 ATES, even when subsequently applied, is low.

597

598 3.6 Climate impact assessment

599 In the E-USE(aq) pilots, enough data have been acquired to calculate yearly equivalent CO₂-emission reductions
600 according to the methodology presented above. Table 5 shows the absolute values of yearly equivalent CO₂ reduction for
601 each pilot, and includes also the specific equivalent CO₂ emission reduction, computed on the basis of ATES system size
602 (kW th peak). The Delft and Ham pilots are shown to yield the highest positive environmental impact: this can be
603 explained by the positive contribution given by solar thermal (Delft) and PVT (Ham) in the reduction of fossil fuel
604 consumption for, respectively, heating and heating plus power. Moreover, in both pilots free cooling can be realized. The
605 Nules pilot plant has an intermediate specific CO₂ emission reduction factor, which is produced only by heating. The
606 application of ATES in a swimming pool allows the system to operate at relatively low temperature (35-40 °C), resulting
607 in a high COP for the geothermal heat pump. In contrast, the Bologna pilot has lower performance in heating due to the
608 higher temperature required (50-60 °C), while space cooling is not directly achievable by direct free cooling via
609 groundwater. The combination of lower COP in heating mode and lower Energy Efficiency Ratio (EER) in cooling mode
610 explains the limited climate impact of the Italian pilot.

611

612 Table 5. Evaluation of yearly equivalent CO₂ emission reduction for E-USE(aq) pilot plants.

Pilot plant	Yearly equivalent CO₂ emission reduction (ton/year)	Yearly equivalent CO₂ emission reduction per installed kW th peak (ton/year)
Nules	25	0.23
Bologna	17	0.11
Delft	25	0.36
Ham	205	0.31

613

614 The analysis offers an indication of the future avoided emissions which can be achieved by wider ATES application.
615 Taking into account experiences with systems in other countries, an average of 0.2-0.3 ton of equivalent CO₂/year per
616 kW th peak is assumed to be a representative GHG mitigation potential value per ATES systems. The CO₂ emission
617 reduction can be further increased if ATES is combined with PV, PVT or wind turbines plants, or if certified “green
618 power” is consumed, since in that case the power feeding the ATES system can be considered as free from CO₂ emissions.

619

620 **4. Conclusions and recommendations**

621 This paper confirms the preliminary conclusions (Pellegrini et al., 2019a) obtained by the EIT Climate-KIC project
622 ‘Europe-wide Use of Sustainable Energy from aquifers’ and adds the following key findings from the six full scale ATES
623 pilots across five European countries:

624 (1) The use of state-of-the-art soil investigation technology can play a powerful role in ATES implementation. Subsurface
625 characterization is essential both for location and design (with appropriate layers selection and optimal spacing between
626 wells) and for effective operation of ATES systems. With proper site characterization, as demonstrated in the pilots, it is
627 possible to apply ATES in relatively thin water bearing layers,.. This makes ATES applicable in parts of Europe that were
628 formerly not considered suitable, included arid regions.

629 (2) Use of thermal energy from ATES can be balanced and optimized more cost efficiently by interlinking with different
630 functions, such as housing, office buildings and industrial activities, as illustrated in several of the pilots. Within a smart
631 grid, ATES is especially compatible with solar energy and heat and cooling from surface water, which provides additional
632 energy that can be stored in the subsoil for later use. This makes ATES also applicable in regions with unequal annual
633 demands for cooling and heating.

634 (3) The presence of soil contamination does not represent an obstacle for ATES application, since ATES can be
635 implemented together with bioremediation. In cases where ATES is economically feasible, groundwater remediation can
636 therefore be made financially more attractive. Thus, soil contamination could even become a driver for the application of
637 ATES.

638 It can therefore be concluded that ATES technology is widely applicable, and its role can become much more prominent
639 amongst the sustainable energy sources required to transition to a low carbon energy system. These results have provided
640 the technical and economic data which may help in overcoming organizational and social acceptance barriers for future
641 ATES systems, thus paving the way to Europe- and even worldwide application. The 6 ATES pilots have illustrated a
642 range of integration challenges, some technical and some commercial/regional, and demonstrated the combination of
643 fields of expertise required to implement solutions that are both economically viable and environmentally beneficial.

644

645 **Acknowledgments**

646 The authors acknowledge the EIT Climate-KIC Association of the European Institute of Innovation and Technology (EIT)
647 that co-financed the barrier analysis, part of the site characterization in the pilot sites as well as part of the monitoring
648 work described in the paper via the E-USE(aq) project. EIT Climate-KIC is a European knowledge and innovation
649 community working towards a climate-resilient society founded on a circular and zero-carbon economy. The authors also
650 wish to thank end users and local authorities who made pilot implementation possible: Emilia Romagna Region, Capital
651 Region of Denmark, Municipalities of Nules, Utrecht & Zwolle as well as Nike & Terna SpA.

652

653 **References**

- 654 Averfalk, H., Werner, S., Felsmann, C., Ruhling, K., Wiltshire, R., Svendsen, S., 2017. Annex XI final report.
655 Transformation Roadmap from High to Low Temperature District Heating Systems.
- 656 Bertani, R., 2005. World Geothermal Generation 2001-2005: State of the Art. In: Proceedings of the World Geothermal
657 Congress, Antalya, Turkey, 24-29 April.
- 658 Bloemendal, M., Hartog, N., 2018. Analysis of the impact of storage conditions on the thermal recovery efficiency of
659 low-temperature ATES systems. *Geothermics* 71, 306–319.
- 660 Bloemendal, M., Olsthoorn, T., van de Ven, F., 2015. Combining climatic and geo-hydrological preconditions as a method
661 to determine world potential for aquifer thermal energy storage. *Sci. Total Environ* 538, 621-633.
- 662 Bonte, M., 2015. Impacts of Shallow Geothermal Energy on Groundwater Quality. Gildeprint Enschede, Amsterdam.
- 663 CBS, 2009. <https://www.cbs.nl/nl-nl/maatwerk/2009/49/warmte-koudeopslag-per-provincie-in-2008--update-tabel-6-2-2-duurzame-energie-in-nederland-2008-->. Accessed date: June 2009.
- 664
- 665 Conti, P., Pellegrini, M., Falcone, G., 2019. Application of the UNFC classification to open-loop ground source heat
666 pump systems: a case study. Proceedings of European Geothermal Congress, The Hague, 11-14 June.
- 667 Douhty, C., Hellstrom, G., Tsang, C.F., 1982. A dimensionless approach to the thermal behavior of an aquifer thermal
668 energy storage system. *Water Resour. Res.* 18, 571–587.
- 669 Dutch soil quality recovery guidelines. <https://www.bodemrichtlijn.nl/Bibliotheek/bodemsaneringstechnieken/a-overzichten/overzicht-factsheets-bodemsaneringstechnieken>. Accessed date: December 2019.
- 670
- 671 Fleuchaus, P., Godschalk, B., Stober, I., Blum, P., 2018. Worldwide application of aquifer thermal energy storage – A
672 review. *Renew. Sust. Energ. Rev.* 94, 861-876.
- 673 Gao, L., Zhao, J., An, Q., Wang, J., Liu, X., 2017. A review on system performance studies of aquifer thermal energy
674 storage. *Energy Procedia* 142, 3537-3545.

675 Haehnlein, S., Bayer, P., Blum, P., 2010. International legal status of the use of shallow geothermal energy. *Renew. Sust.*
676 *Energ. Rev.* 14, 2611-2625.

677 Hausner, M.B., Suárez, F., Glander, K.E., van de Giesen, N., Selker, J.S., Tyler, S.W., 2011. Calibrating Single-Ended
678 Fiber-Optic Raman Spectra Distributed Temperature Sensing Data. *Sensors* 11, 10859–10879.

679 Hoekstra, N., van Gelderen, M., 2019. E-USE(aq) Project website. [https://www.deltares.nl/en/projects/europe-wide-use-](https://www.deltares.nl/en/projects/europe-wide-use-soil-energy-ates/)
680 [soil-energy-ates/](https://www.deltares.nl/en/projects/europe-wide-use-soil-energy-ates/). Accessed date: December 2019.

681 Koenders, M., 2015. Meer met Bodemenergie research program. <http://meermetbodemenergie.nl>, Accessed date:
682 December 2015.

683 Koffi, B., Cerutti, A., Duerr, M., Iancu, A., Kojna, A., Janssens-Maenhout, G., 2017. CoM Default Emission Factors for
684 the Member States of the European Union, European Commission, Joint Research Centre (JRC).

685 Kontu, K., Rinne, S., Junnila, S., 2019. Introducing modern heat pumps to existing district heating systems – Global
686 Lessons from viable decarbonizing of district heating in Finland. *Energy* 166, 862-870.

687 Lund, H., Werner, S., Wiltshire, R., Svendsen, S., Thorsen, J.E., Hvelplund, F., 2014. 4th Generation District Heating
688 (4GDH); integrating smart thermal grids into future sustainable energy systems. *Energy* 68, 1–11.

689 Monti, M., Meggiolaro, M., Matthews, D., Angelino, L., Dumas, P., Mendrinós, D., Raftegard, O., Giambastiani, B.M.S.,
690 Mastrocicco, M., 2012. Regional strategies for the large scale introduction of geothermal energy in buildings – The results
691 of GEO.POWER project. Ferrara: Le Immagini Edizioni.

692 Mellor, A., Alonso Alvarez, D., Guarracino, I., Ramos, A., Riverola Lacasta, A., Ferre Llin, L., Murrell, A.J., Paul, D.J.,
693 Chemisana, D., Markides, C.N., Ekins-Daukes, N.J., 2018. Roadmap for the next-generation of hybrid photovoltaic-
694 thermal solar energy collectors. *Sol. Energy* 174, 386-398.

695 NVOE (Richtlijnen Ondergrondse Energieopslag), 2006. Design Guidelines of Dutch Branch Association for Geothermal
696 Energy Storage. Woerden.

697 Pellegrini, M., Bloemendal, M., Hoekstra, N., Spaak, G., Andreu Gallego, A., Rodriguez Comins, J., Grotenhuis, T.,
698 Picone, S., Murrell, A.J., Steeman, H.J., 2019. Low carbon heating and cooling by combining various technologies with
699 Aquifer Thermal Energy Storage. *Sci. Total Environ.* 665, 1-10.

700 Pellegrini, M., Bianchini, A., Guzzini, A., Saccani, C., 2019. Classification through analytic hierarchy process of the
701 barriers in the revamping of traditional district heating networks into low temperature district heating: an Italian case
702 study. *Int. J. Sust. Energ. Plann. Manag.* 20, 51-66.

703 Schüppler, S., Fleuchaus, P., Blum, P., 2019. Techno-economic and environmental analysis of an Aquifer Thermal Energy
704 Storage (ATES) in Germany. *Geot. Energ.* 7, 1-24.

705 Schmidt, T., Pauschinger, T., Sørensen, P.A., Snijders, A., Djebbar, R., Boulter, R., Thornton, J., 2018. Design Aspects
706 for Large-scale Pit and Aquifer Thermal Energy Storage for District Heating and Cooling. Energy Procedia 149, 585-
707 594.

708 Short, W., Packey, D., Holt, T., 1995. A Manual for the Economic Evaluation of Energy Efficiency and Renewable
709 Energy Technologies, NREL/TP-462e5173.

710 Sommer, W., Valstar, J., Leusbrock, I., Grotenhuis, T., Rijnaarts, H., 2015. Optimization and spatial pattern of large-scale
711 aquifer thermal energy storage. Appl. Energy 137, 322–337.

712 van Agt, J., 2011. <http://www.olino.org/articles/2011/09/19/warmtepomp-vs-gasketel>. Accessed date: December 2019.

713 van Beek, C.G.E.M., 2010. Cause and prevention of clogging of wells abstracting groundwater from unconsolidated
714 aquifers. PHD thesis, Vrije Universiteit Amsterdam.

715 Werner, S., 2017. International review of district heating and cooling. Energy Procedia 137, 617-631.